Bulletin of the New Zealand Society for Earthquake Engineering, Vol. 48, No.2, June 2015

TECHNICAL NOTE

SHAKING TABLE TESTS OF A BASE ISOLATED STRUCTURE WITH DOUBLE CONCAVE FRICTION PENDULUM BEARINGS

Felice C. Ponzo[1], Antonio D. Cesare[2], Gianmarco Leccese[3] and Domenico Nigro[2]

(Submitted as Paper *June 2014*; Reviewed *September 2014*; Accepted as Technical Note *April 2015*)

ABSTRACT

An extensive experimental testing programme named JETBIS project (Joint Experimental Testing of Base Isolation Systems) was developed within the RELUIS II project (Task 2.3.2) and RELUIS III project (Line 6) involving partners from different Italian universities. This paper describes the seismic tests performed by the research unit of University of Basilicata (UNIBAS) on an isolation system based on Double Concave Friction Pendulum (DCFP) bearings. The DCFP bearing contains two separate concave sliding surfaces and exhibits different hysteretic properties at different stages of displacement response. The main objective of this work is to evaluate the horizontal response of the DCFP isolators by means of controlled-displacement tests and shaking table tests. The experimental model was a 1/3 scaled steel framed structure with one storey and one bay in both directions. Four DCFP bearings with equal properties of the sliding surfaces were considered. In this work, three different sliding surface conditions (with and without lubrication) have been studied. The isolated base model was subjected to 8 natural earthquakes of increasing seismic intensities and considering two mass configurations (with both symmetrical and eccentric masses). The reliability of the design procedure considered for the isolation system was verified also when relevant residual displacements occurred due to previous earthquakes. In this paper, the comparisons between the experimental outcomes and the numerical results of nonlinear time-history analyses using SAP2000 are shown.

INTRODUCTION

The underlying concept of base isolation is the uncoupling of the horizontal building movement from ground motions using a flexible isolation layer made with either elastomeric (rubber) or sliding bearings [1]. Sliding isolators use friction between composite materials, usually composed of polyethylene and stainless steel plates providing friction properties as their energy dissipation mechanism. The effectiveness of the isolation systems based on flat surface sliders combined with anti-seismic devices has been proven by various experimental campaigns and also the research conducted at UNIBAS [2].

Theoretical and experimental research studies were focused on developing more versatile and economic isolation systems such as the friction pendulum [3]. The friction pendulum bearing (FPS), proposed by Zayas *et al.* [4] is a sliding seismic isolation system which uses its surface curvature to generate the restoring force from the pendulum action of the weight N of the superstructure on the FPS (Figure 1a). The idealized bilinear cyclic behaviour of FPS bearing, with radius R and friction coefficient μ, is shown in Figure 1b: friction force F_0 at zero displacement, restoring stiffness K_r and the lateral force F at the displacement d are defined by Equation 1.

$$F_0 = N \cdot \mu \, , K_r = \frac{N}{R}$$

$$F = F_0 + K_r \cdot d \qquad (1)$$

The main properties of FPS are that the fundamental period of vibration of the isolated structure is independent from the mass M of the superstructure, it depends only on the radius of the sliding surface R [5], while the effective damping depends also on the current lateral displacement d (at angle θ) and sliding friction coefficient μ. The fundamental period T and the equivalent viscous damping ξ_{eq} of FPS are equal to Equation 2, where g is the gravity acceleration.

$$T = 2\pi \sqrt{\frac{M}{K_r}} = 2\pi \sqrt{\frac{R}{g}}$$

$$\xi_{eq} = \frac{2}{\pi} \cdot \frac{\mu \cdot R}{d} \qquad (2)$$

A remarkable improvement of the performance of the FPS isolator is obtained by introducing a second sliding surface (Figure 1c). The Double Concave Friction Pendulum (DCFP) bearing consists of two steel concave plates separated by a double friction slider, which produce two independent pendulum response mechanisms. The DCFP bearing allows reaching greater maximum displacement, given by $d_{max} = 2u$ (Figure 1c), compared to a corresponding FPS with the same dimensions in plan. Moreover, there is the capability to use sliding surfaces with varying radii of curvature and coefficients of friction, offering the designer greater flexibility to optimize performances of the isolation system [6].

[1] *Corresponding Author, Associate Professor, School of Engineering, University of Basilicata, Potenza, Italy, felice.ponzo@unibas.it*
[2] *School of Engineering, University of Basilicata, Potenza, Italy.*
[3] *Graduate Student, School of Engineering, University of Basilicata, Potenza, Italy.*

When a DCFP bearing having the same coefficient of friction for the upper and lower surfaces ($\mu = \mu_1 \approx \mu_2$) and sliding occurring simultaneously on both surfaces (Figure 1c) it can be modeled as a combination in series of two FPS with equivalent radius R_{eq} equal to the sum of the radii of curvature ($R_{eq} = R_1+R_2$) [1, 5, 7].

In the case of equal radii ($R_1=R_2$), the idealized cyclic behaviour resembles the functioning of the DCFP bearings and consists of a bi-linear force-displacement equal to that of the FPS (Figure 1b).

This paper briefly describes the experimental testing carried out on DCFP bearings with a rigid slider, an equal radius of curvature and the same friction coefficient on both sliding surfaces. Three different conditions of the sliding surfaces (Low, Medium and High friction), obtained with and without lubrication, have been tested by means of controlled-displacement and seismic-input experiments performed using the uni-directional shaking table at UNIBAS and at University of Naples "Federico II" (UNINA), respectively. In this paper the results of nonlinear time-history analysis carried out using the finite element programme SAP2000 [8] are compared with experimental outcomes.

EXPERIMENTAL INVESTIGATIONS

Experimental Model

In the JETBIS project a steel framed structure was designed as an inverted pendulum, see Figure 2, and was considered as the benchmark structure to simulate the seismic effects at a generic building as an equivalent single degree of freedom (SDOF) system.

The benchmark test frame is one-storey and one bay in both directions, storey height is 2.9 m and the plane dimensions are 2.5 x 2.0 m. It is composed of welded square hollow columns (150 x 150 x 15 mm) of C45 steel material (minimum yield strength of about 340 MPa) and rolled square hollow beams (120 x 120 x 12.5 mm) of S275 steel (minimum yield strength of about 275 MPa). The beam-column connections are bolted. A 250 mm thick reinforced concrete slab of class C45/55 (concrete compressive cylinder strength 45 MPa) is placed on the roof of the structure. The fundamental period of the fixed base structure is 0.26 sec, estimated by means of dynamic identification tests [9].

A rigid floor base consisting of a horizontal braced steel frame with HEM160 section for external primary beams and UPN80 section for internal secondary beams was added to the benchmark model. Additional masses of concrete blocks (23.8 kg each) were placed on the base floor. The isolated model became a two degrees of freedom (2DOF) system in the test direction, corresponding to the two horizontal floor displacements where the structural mass is concentrated (see Table 1).

In this project the isolated model was considered as scaled 1:3, in order to reduce the maximum displacement coherently with the limits of the test facility. Consequently, the effects on the superstructure were not relevant.

Seismic loads were applied parallel to the long side of structure (longitudinal direction), as shown in Figure 2a. During the seismic tests two different mass configurations of the isolated model have been considered, changing the number and position of concrete blocks on the base level (see Figure 2b), assuming: Centered masses (C) with 40 blocks and Eccentric masses (E) with 38 blocks plus steel plates. The total eccentricity perpendicular to the text direction $e_{tot,x}$ is the distance between the stiffness centre of the isolation system, assumed coincident to geometrical centre, and the vertical projection of the centre of mass of the superstructure. The total eccentricity $e_{tot,x}$ is calculated using Equation 3, where m_i and $e_{i,x}$ are the mass and the mass eccentricity of the i-th storey. Mass eccentricity and the percentage of the length of the superstructure transverse to the load direction are summarized in Table 1. Figure 2c shows an overview of the experimental model on the shaking table.

$$e_{tot,x} = \frac{\sum_i m_i \cdot e_{i,x}}{m_{tot}} \tag{3}$$

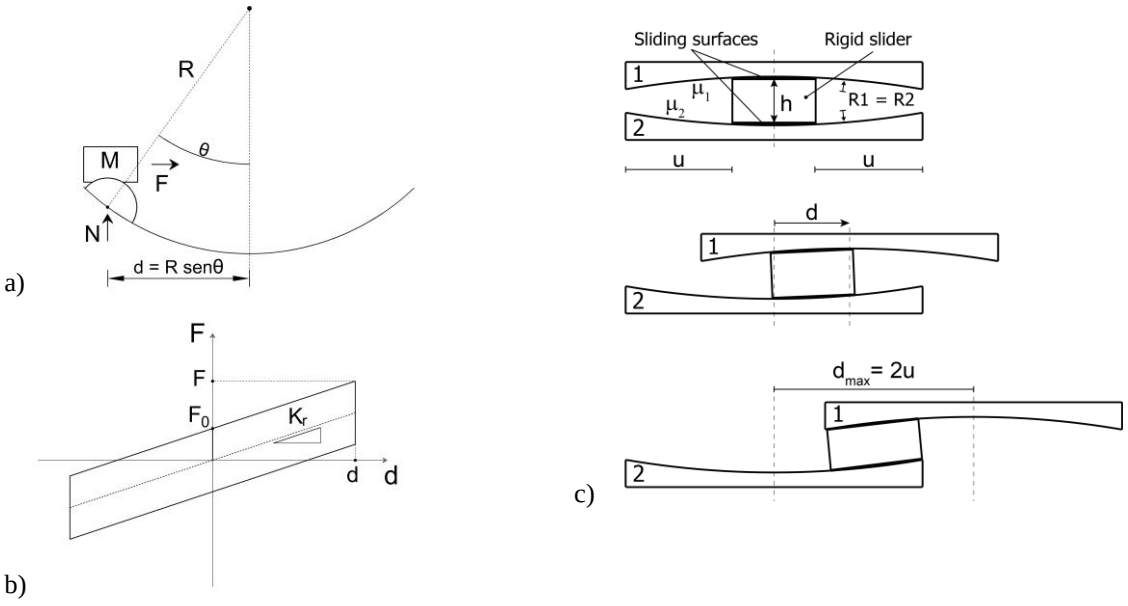

Figure 1: a) Functioning principles of FPS; b) idealized bilinear cyclic behaviour; c) functioning scheme of the DCFP bearing.

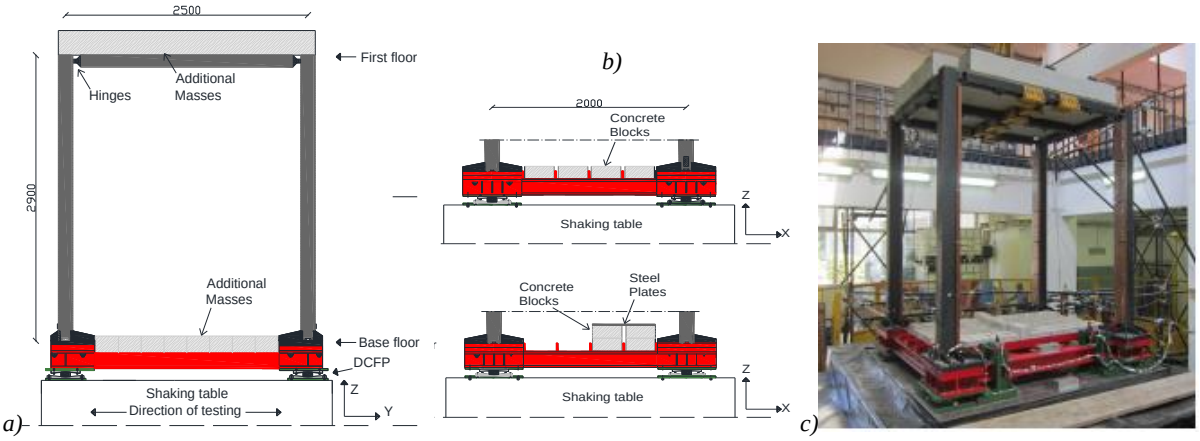

Figure 2: a) Longitudinal view of the experimental model; b) Transversal views of the base isolated; c) Overview of the experimental model.

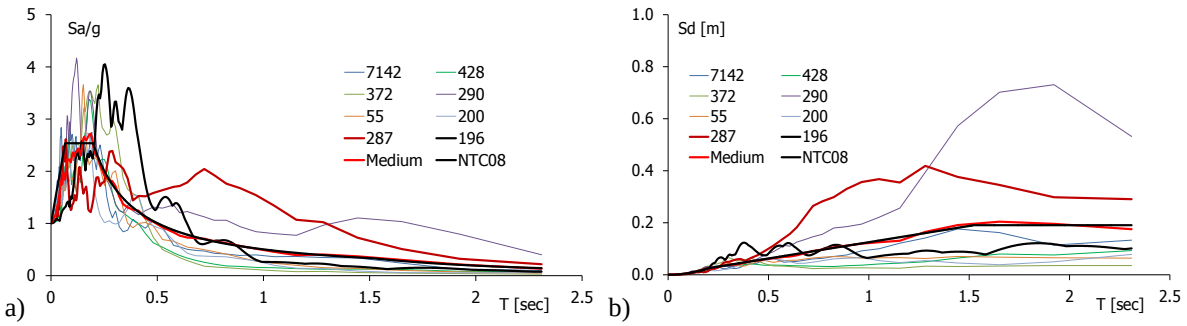

Figure 3: Normalized elastic spectra of the seismic inputs: a) accelerations and b) displacements.

Table 1: Masses of experimental model.

Storey	Centred Masses (C)	Eccentric Masses (E)		
	m_i [t]	m_i [t]	$e_{i,x}$ [mm]	$p_{i,x}$ [%]
Base	3.20	3.80	150	7%
1st floor	5.00	5.00	0	0%
Total	8.20	8.80	65	3%

Table 2: Seismic inputs selected for experimental testing.

Waveform ID	Earthquake Name	Date	Mw	PGA ref. [ag/g]	Soil
7142	Bingol	01/05/2003	6.3	0.25	A
55	Friuli	06/05/1976	6.5	0.25	A
200	Montenegro	15/04/1979	6.9	0.25	A
428	Etolia	18/05/1988	5.3	0.25	A
372	Lazio-Abruzzo	07/05/1984	5.9	0.25	A
290	Campano Lucano	23/11/1980	6.9	0.25	A
287	Campano Lucano	23/11/1980	6.9	0.25	A
196	Montenegro	15/04/1979	6.9	0.45	B

Seismic Inputs

The seismic inputs considered in the JETBIS project were a set of 7 natural earthquakes with the mean spectrum compatible with soil type A, and 1 natural earthquake compatible with soil type B, as defined by seismic codes (NTC [10]; EC8-1 [11]; NZS-1170.5 [12]). All accelerograms were selected from the *European Strong Motion Database* (ESD) [13], in Table 2 the main characteristic (Magnitude Mw, reference Peak Ground Acceleration (PGA) and Soil class) are summarized. The normalized elastic spectra of accelerations and of displacements are reported in Figure 3. To ensure consistency with the scale of the experimental model, the design spectrum was scaled down in periods by a factor of $1/\sqrt{3}$.

Design of Isolation System

The design method considered to define the main properties of the DCFP bearings is based on the simplified linear analysis assuming the superstructure as a rigid solid translating above the isolation system [11]. DCFP bearings with equal radius of curvature ($R_1 = R_2$) and the same friction coefficient ($\mu_1 \approx \mu_2$) were considered in the design. The equivalent linear model shown in Figure 4a was used for the design of DCFP isolation system. The effective stiffness K_{eff} of the isolation system is the secant value of the stiffness at the design displacement $d_{dc.}$ The effective stiffness K_{eff} and the effective period of translation T_{eff} are evaluated with Equations 4, where N_{Ed} is the design vertical load in the seismic condition. The effective damping ξ_{eff} is expressed by Equations 5. The design friction coefficient μ is one of the main design parameters [14]. It influences directly the damping but also the residual displacement. Generally, the manufacturer can supply different sliding materials, the designer can choose the conditions of the sliding surfaces, in a range of values given by manufacturer, and if required, lubricate them.

$$K_{eff} = N_{Ed} \cdot \left(\frac{1}{R_{eq}} + \frac{\mu}{d_{dc}} \right)$$

$$T_{eff} = 2\pi \sqrt{\frac{M}{K_{eff}}} = 2\pi \sqrt{\frac{1}{g \cdot \left(\frac{1}{R_{eq}} + \frac{\mu}{d_{dc}} \right)}} \quad (4)$$

$$\xi_{eff} = \frac{2}{\pi} \cdot \frac{\mu \cdot M \cdot g}{K_{eff} \cdot d_{dc}} = \frac{2}{\pi} \cdot \frac{1}{\frac{d_{dc}}{\mu \cdot R_{eq}} + 1} \quad (5)$$

The design procedure was applied for the case of centred masses (N_{Ed} = 80.44 kN) and the earthquake ID 287 (one of largest earthquakes for long-period structure) varying the design displacement d_{dc}, consequently the effective stiffness K_{eff} and the effective damping ξ_{eff}, until the difference between assumed and calculated values of d_{dc} does not exceed 5% of the assumed value. The maximum value of effective damping ξ_{eff} < 28% [10] is assumed in the design. In Figure 4b are shown the accelerations and displacements spectra of the earthquake 287 with PGA = 0.5g (200% of the PGA ref, see Table 2) reduced by different values of damping. Figure 4b reports also the effective period and the accelerations and displacements obtained by the iterative procedure for Low friction (μ = 2.5%), Medium friction (μ = 5%) and High friction (μ = 12%) coefficients.

DCFP Bearings

The seismic isolation system consisted of four "small-size" DCFP bearings, one under each column, as shown in Figure 2, both accommodating horizontal displacements and rotations about the vertical axes. Bolts were used to ensure a rigid connection between the isolators and the basement of the test model. In this application, each DCFP bearing consists of two identical concave sliding surfaces having an external diameter 300 mm, radii of curvature $R_1 = R_2$ = 925 mm and a rigid slider with a diameter of 75 mm and height 45 mm (Figure 5). An Ultra-High Molecular Weight Poly-Ethylene (UHMW-PE) high bearing capacity composite material produced by FIP [15] covers the rigid slider. The sliding material is essential to give stability to the hysteretic force vs. displacement curves with displacement and velocity. In lubricated condition, a silicone based lubricant (lithium soap) was applied to the top and bottom face of the rigid slider. The equivalent radius of curvature of the DCFP isolator unit is R_{eq} = 1,805 mm, approximately twice the geometric radius of curvature of each sliding surface taking into account the distance from the centre of the spherical surface to the pivot point of the articulated slider. The overall displacement capacity is $d_{max} = 2\ u = \pm 180$ mm, see Figure 1c.

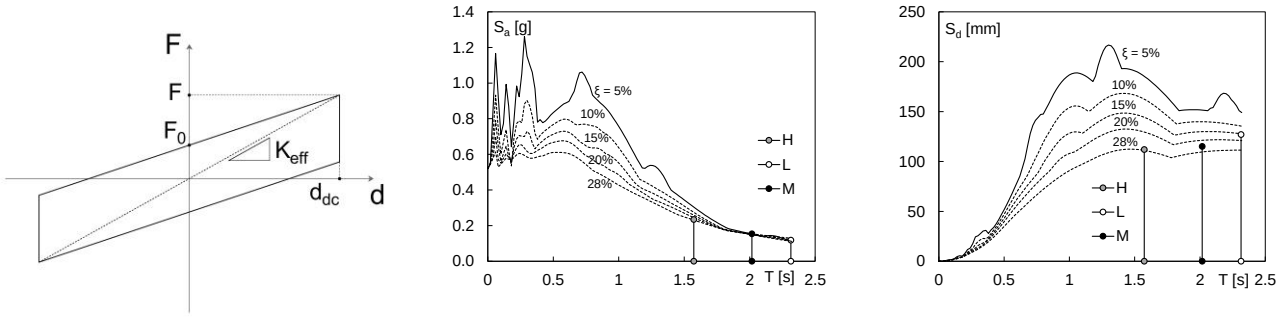

a) b)

Figure 4: a) Equivalent linear model of DCFP considered in the design, b) Design reference spectra of acceleration and displacement.

Figure 5: Overview of the DCFP bearing.

NUMERICAL MODELLING

The steel frame was modelled using frame-type 3D finite elements (Figure 6a) in SAP2000. The connection between the columns and the stiff beams at the base of the model was simulated through the use of fixed restraints with the floor slabs being simulated by imposing a rigid diaphragm assumption. The DCFP bearings have been modelled by using one joint link element type biaxial Friction-Pendulum Isolator, see Figure 6a. In SAP2000 the friction and restoring forces are directly proportional to the compressive axial force in the element which cannot carry axial tension. The cyclic nonlinear behaviour of the DCFP isolator unit has been modelled with the initial stiffness K_i (before sliding), as shown in Figure 6b [8].

The velocity dependence of the coefficient of friction is described by Equation 6 [16], where v is the sliding velocity, μ_{fast} and μ_{slow} are the sliding coefficients of friction at slow and fast velocity, respectively and α is a rate parameter that controls the transition from μ_{slow} to μ_{fast}. The numerical models of DCFP bearings having different sliding surface conditions have been calibrated against the results of the displacement-controlled testing.

$$\mu = \mu_{fast} - (\mu_{fast} - \mu_{slow}) \cdot e^{-\alpha \cdot |v|} \tag{6}$$

EXPERIMENTAL AND NUMERICAL RESULTS

Displacement-controlled Tests

Characterization testing of a DCFP bearing has been performed to confirm the theoretical predictions. The testing machine available at UNIBAS consists of one horizontal actuator and two vertical actuators and is capable of testing bearings under controlled conditions of vertical load, lateral movement and rotational movement. Load cells mounted directly beneath the actuators measure reaction forces and lateral displacement is measured by an internally mounted LVDT on the horizontal actuator.

Three different conditions of surfaces have been considered, as follows:

1. High friction (H), as standard condition of surfaces without lubrication;
2. Low friction (L), obtained with lubricated surfaces;
3. Medium friction (M), obtained by cleaning the lubricated surfaces.

The four bearings were tested together under a vertical compressive load N = 128 kN, which represents the minimum value available of the test machine. A series of sinusoidal lateral displacements were imposed with a slow sliding velocity (v = 50 mm/s) and a fast sliding velocity (v = 400 mm/s) in accordance with Eurocode [17]. Figure 7 shows the experimental force-displacement relationships of the DCFP bearings and the numerical results. The experimental results of the fast velocity testing of High friction present some little bumps corresponding to the inversion of the direction of motion due to the inertial effects of the test machine with respect to the relatively small vertical load applied. A good agreement with experimental outcomes was observed when initial stiffness K_i, friction coefficients μ_{fast} and μ_{slow} and rate parameter α assume the values reported in Table 3.

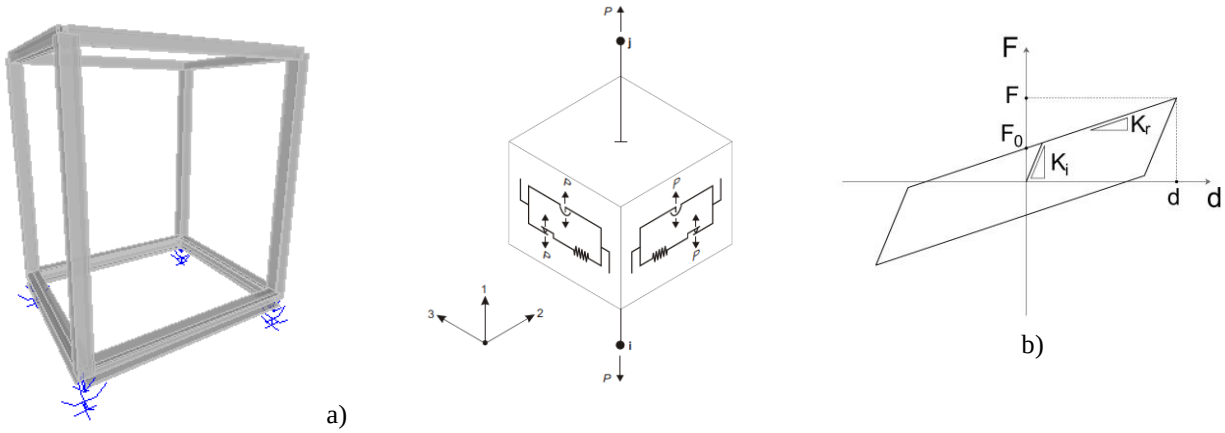

Figure 6: a) Numerical model of the experimental steel frame and of the DCFP isolator unit (SAP 2000, 2013); b) nonlinear cyclic behaviour of the DCFP bearings.

Table 3: Numerical parameters of DCFP selected on the basic of controlled-displacement test results.

Surfaces condition	K_i [kN/m]	μ_{slow} [%]	μ_{fast} [%]	α [s/m]
High friction (H)	5000	12	20	5.0
Low friction (L)	5000	2.5	5	5.0
Medium friction (M)	5000	5	8	5.0

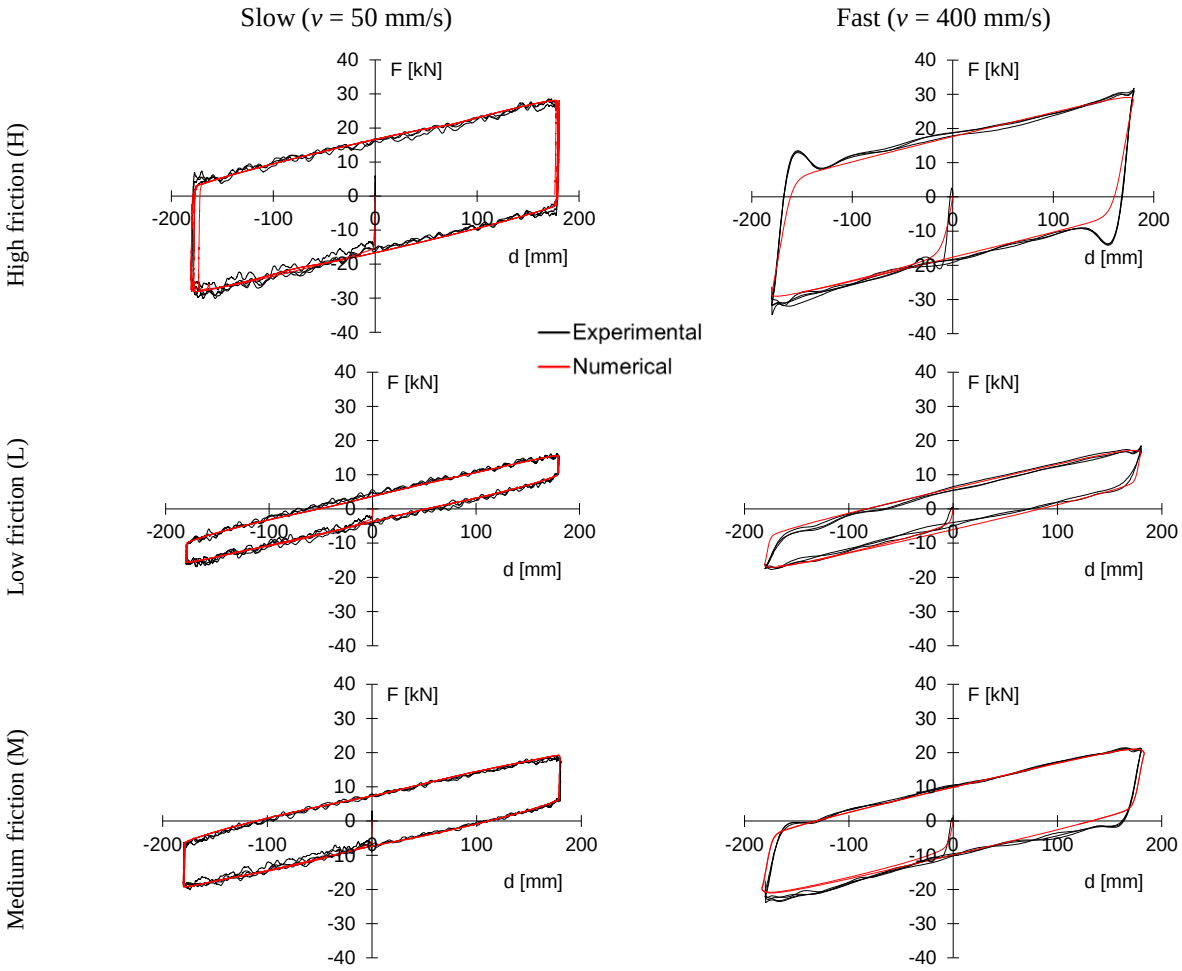

Figure 7: Experimental and numerical cyclic Force–displacement behaviour of four DCFP bearing.

Table 4: Experimental configurations for shaking table tests.

Experimental configuration	Experimental Model mass configuration	Surfaces Condition of DCFP bearings
C-H	Centred masses	High friction (H)
C-L	Centred masses	Low friction (L)
C-M	Centred masses	Medium friction (M)
E-M	Eccentric masses	Medium friction (M)

Shaking Table Tests

Four experimental configurations have been considered, as reported in Table 4, for a total of 61 shaking table tests. During testing the PGA of the seismic input was increased in value until a design value of 200% PGA_{ref} was reached (PGA ref, see Table 2). The seismic response was recorded by a total of 16 servo-accelerometers and 14 displacement transducers.

In order to evaluate the influence of the residual displacements on the maximum values, in Figure 8 the experimental values of initial, maximum and residual displacements of the base isolation system are reported as tested chronologically. In the C-H configuration (standard condition of surfaces) the isolation system responded in a different manner with and without initial residual displacements. In the case of C-L configuration (applying the lubrication) the displacements of the isolation system increased by about 10% and no residual displacements were recorded. The C-M configuration (Cleaning the lubrication) shows similar maximum displacements with respect the C-H case. The case of eccentric masses (E-M) shows a difference between the maximum experimental displacements with centred masses (C-M) less than 5%. The distance between the centre of mass and the centre of stiffness of the isolation system is null due to the axial load dependency of the stiffness on the DCFP isolator unit. Therefore the torsional effects are negligible.

Comparison of Results

In Figure 9 the experimental results are compared with the results of the design procedure for all model configurations subjected to the seismic input 287 at all tested PGA in terms of the maximum base displacements *d* and the ratio between

the maximum acceleration at the base a_{bas} and the table acceleration a_{tab}. As can be seen, the experimental maximum displacements are similar to the design predictions and the acceleration ratio is almost always less than unity and decreases when the PGA increased. No influence of initial displacements can be highlighted in the case of C-H configuration. The displacements from design procedure are smaller than the experimental ones for all configurations of PGA greater than 100%.

Figure 10 and Figure 11 display the experimental and numerical time-histories of base displacement and base acceleration of C-H, C-L and C-M configurations when earthquake ID 287 with PGA = 0.5g and earthquake ID 196 with PGA = 0.9g (PGA 200%) were applied. A good agreement between the shaking table results and the results of nonlinear time-history analysis carried out with the numerical model of the DCFPs, reported in Table 3 (see also Figure 6), was obtained for all test model configurations.

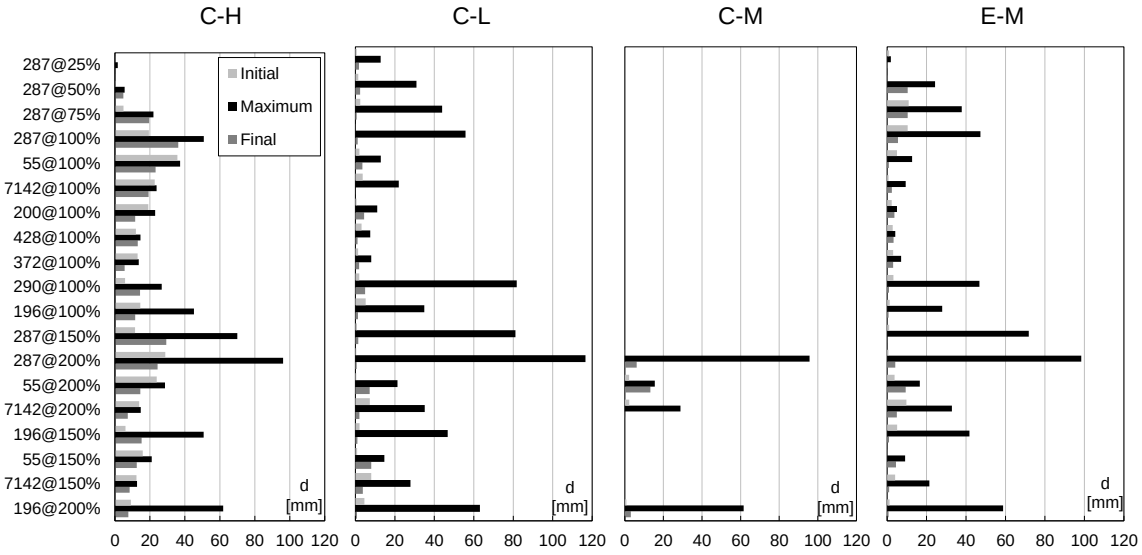

Figure 8: Experimental base displacements of all tests: initial, maximum and residual.

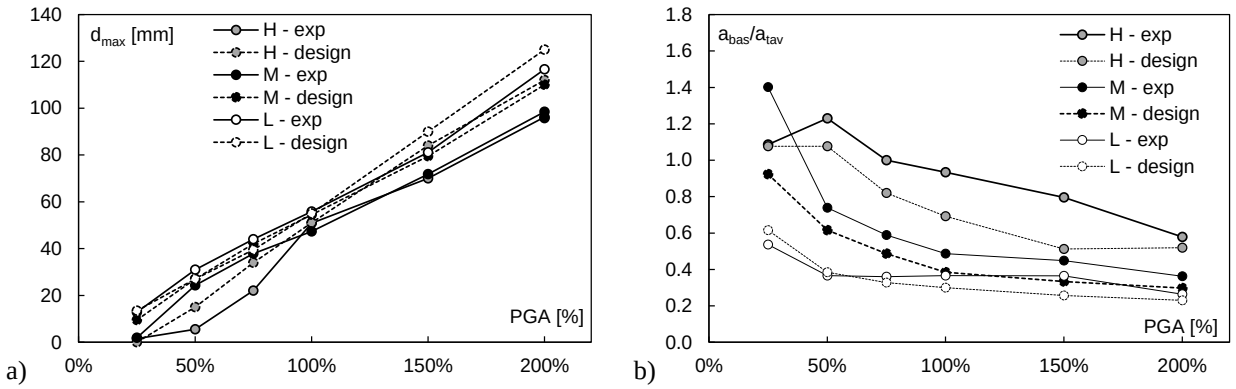

Figure 9: Experimental results and design predictions for Centred masses C and earthquake ID 287: a) maximum base displacement and b) ratio between maximum base and maximum table accelerations.

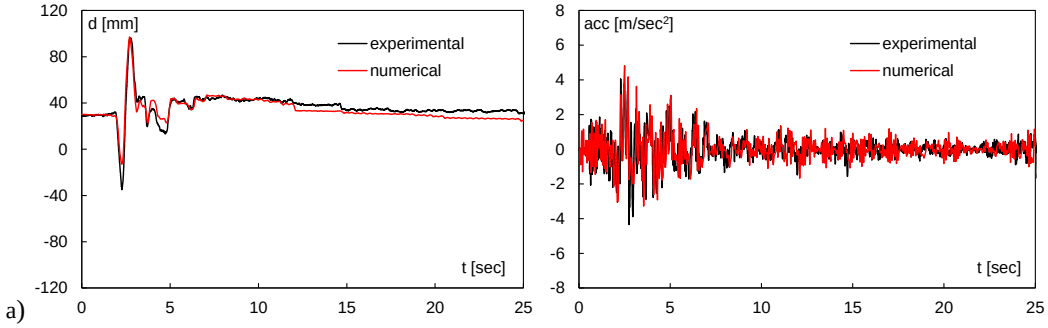

Figure 10: Experimental and numerical time histories of displacement and acceleration for earthquake 287 at PGA 200% for model configuration a) C-H

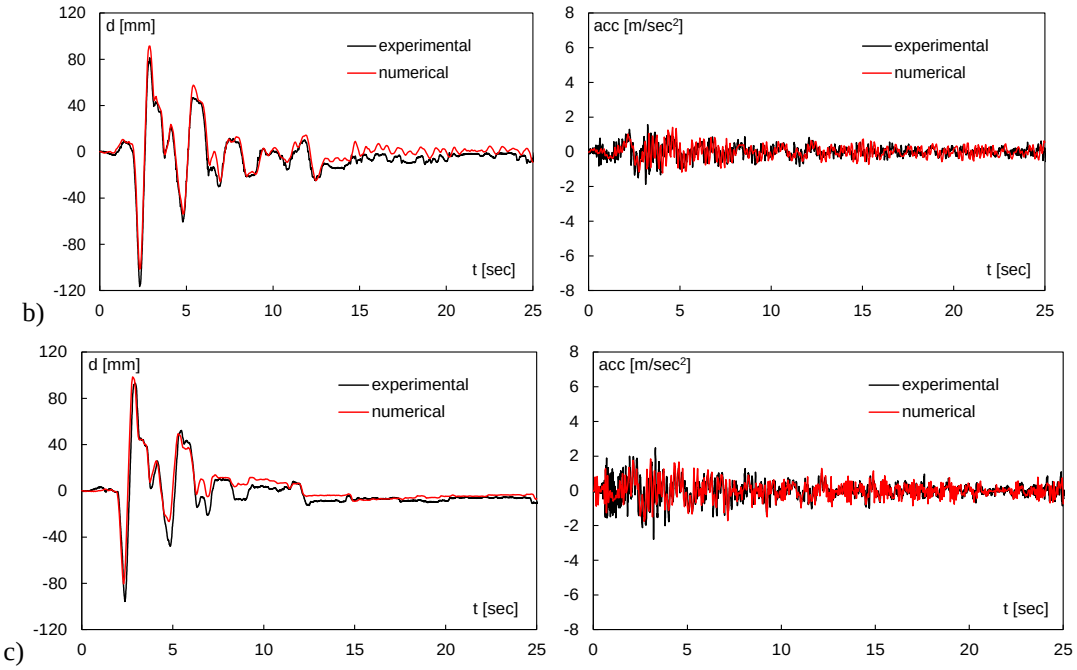

Figure 11 cont.: Experimental and numerical time histories of displacement and acceleration for earthquake 287 at PGA 200% for model configuration b) C-L and c) C-M.

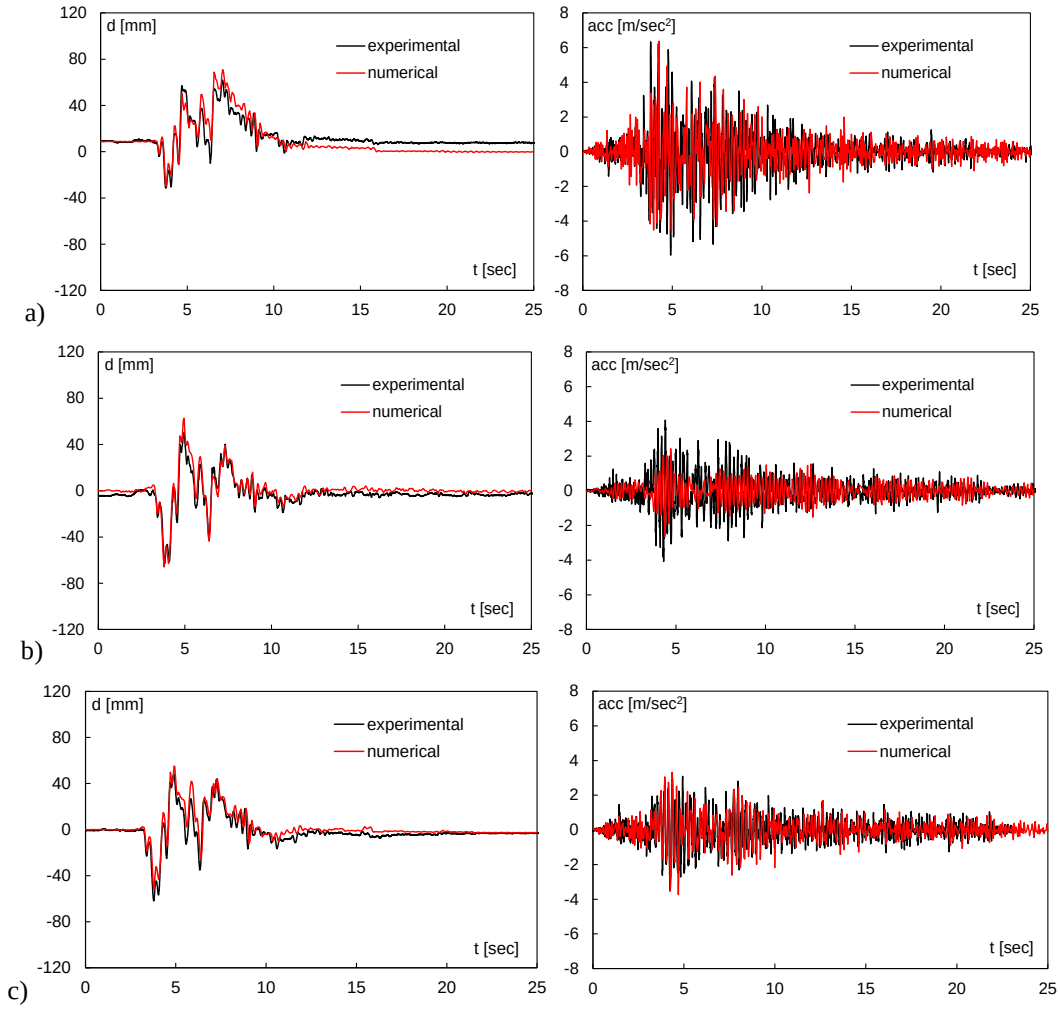

Figure 12: Experimental and numerical time histories of displacement and acceleration for earthquake 196 at PGA 200% for model configuration a) C-H, b) C-L and c) C-M.

CONCLUSIONS

In this paper double concave friction pendulums DCFP with rigid slider and equal radii of curvature have been investigated with lower and upper sliding surfaces having the same friction coefficient. Three different conditions of sliding friction (High, Medium and Low friction) have been considered. The bilinear cyclic behaviour of DCFP bearings were verified through controlled-displacement tests. Moreover, shaking table test have been performed considering different mass configurations of the experimental model, symmetric and eccentric. The experimental results show a stable behaviour of the DCFP bearings under horizontal seismic loading. The design procedure is reliable to adequately predict the displacement demands over many high intensity seismic inputs even when initial slider offsets are present. The maximum displacement reached during testing is independent of the mass configuration and the torsional effects are negligible. The numerical simulations have shown sufficient accuracy to closely track the time-histories of base displacement and acceleration (within 10% error).

ACKNOWLEDGEMENTS

This work was funded by the Italian Department of Civil Protection within the project RELUIS II (2010/13) and RELUIS III (2014). FIP Industriale, Italy, supplied the DCFP bearings. This support is gratefully acknowledged.

REFERENCES

1 Becker TC and Mahin SA (2012). "Experimental and Analytical Study of the Bi-directional Behavior of the Triple Friction Pendulum Isolator". *Earthquake Engineering and Structural Dynamics*, **41**: 355–373.

2 Ponzo FC, Di Cesare A, Nigro D and Dolce M (2011). "An Update of Innovative Retrofitting Techniques for RC and Masonry Building: from Experimental Investigations to Practical Applications". *Proceedings of the 9th Pacific Conference on Earthquake Engineering* 14-16 April, 2011, Auckland, New Zealand.

3 Dao ND, Ryan KL, Sato F and Sasaki T (2013). "Predicting the Displacement of Triple Pendulum Bearings in a Full-Scale Shaking Experiment Using a Three-Dimensional Element". *Earthquake Engineering and Structural Dynamics*, **42**:1677–1695

4 Zayas VA, Low SS and Mahin SA (1987). *"The FPS Earthquake Resisting System: Experimental Report"*. Report No. UCB/EERC-87/01. Earthquake Engineering Research Center, University of California, Berkeley, USA.

5 Kim YS and Yun CB (2007). "Seismic Response Characteristics of Bridge Using Double Concave Friction Pendulum Bearings with Tri-linear Behaviour". *Engineering Structures*, **29**(11): 3082-3093.

6 Malekzadeh M and Taghikhany T (2010). "Adaptive Behavior of Double Concave Friction Pendulum Bearing and its Advantages over Friction Pendulum Systems". *Civil Engineering*, **17**(2): 81-88.

7 Fenz DM and Constantinou MC (2006). "Behaviour of the Double Concave Friction Pendulum Bearing". *Earthquake Engineering and Structural Dynamics*, **35**:1403-1424.

8 SAP2000 (2013). *"Analysis Reference Manual"*. Computers and Structures Inc., Berkeley, USA.

9 Magliulo G, Petrone C, Capozzi V, Maddaloni G, Lopez P, Talamonti R and Manfredi G (2012). "Shake Table Tests on Infill Plasterboard Partitions". *Open Construction and Building Technology Journal*, **6**(1): 155-163, DOI: 10.2174/1874836801206010155.

10 NTC (2008). "*Italian Technical Code for Constructions (in Italian)".* DM 14/01/2008, Ministry of Infrastructures, Italy.

11 EC8-1 (2004). *Design of Structures for Earthquake Resistance, Part 1: General Rules, Seismic Actions and Rules for Buildings"*. European Standard EN 1998-1, European Committee for Standardization (CEN), Brussel.

12 NZS-1170.5 (2004). *"Structural Design Actions. Part 5: Earthquake Actions – New Zealand – Commentary"*. Supplement to NZS 1170.5:2004, Standards New Zealand, Wellington, NZ.

13 ESD (2008). *"European Commission for Community Research. European Strong Motion Database"* (on-line), http://www.isesd.cv.ic. ac.uk/ESD.

14 Casarotti C and Pavese A (2014). "Statistical Results of a Wide Experimental Campaign on Full Scale Curved Surface Sliders" *Second European Conference on Earthquake Engineering and Seismology*, Istanbul, August 25-29, 2014.

15 FIP INDUSTRIALE SpA (2013). *"Brochure S04: Curved Surface Sliders"*. Padova. http://www.fipindustriale.it

16 Constantinou M, Mokha A and Reinhorn AM (1990). "Teflon Bearings in Base Isolation, Part II: Modeling". *Journal of Structural Engineering*, ASCE, **116**(2): 455–474.

17 CEN (2009). *"UNI EN 15129*: *Antiseismic Devices"*. European Committee for Standardization (CEN), Brussel.